

**Massachusetts Institute of Technology  
Physics Department**

8.13/8.14

1993/1994

Junior Physics Laboratory: Experiment #6

## The Zeeman Effect and Hyperfine Structure in Mercury and Neon

This purpose of this experiment is to measure the Zeeman effects and hyperfine structure in the spectra of mercury and neon by high-resolution spectroscopy with a Fabry-Perot interferometer. Chapter 7 of "Experiments in Modern Physics" by Melissinos (1966) provides an introduction to the theory of the Zeeman effect and hyperfine structure and to Fabry-Perot interferometry. The discussion in this lab guide will be confined mainly to theoretical matters not covered by Melissinos and practical matters unique to the experimental setup in the Junior Lab. Additional background material on the quantum theory of the Zeeman effect and to the physical optics of the interferometer can be found in various texts, in particular those listed in the references at the end of this lab guide.

### PREPARATORY QUESTIONS

1. Draw a diagram that shows the effect of a weak magnetic field on the otherwise degenerate substates involved in the transitions which produce the green line (5461 Å) and the yellow doublet (5770 Å and 5791 Å) of mercury.
2. Derive the Landé  $g$ -factors for the states involved in the production of these lines.
3. What would the Zeeman effect be on the  $\lambda$  5461 Å line if the gyromagnetic ratio of the electron were 1 instead of 2.001?
4. Derive equation (5) in this lab guide. Also derive equation (8) from equation (7).
5. Estimate the Doppler breadth of the  $\lambda$  5461 Å line from the mercury lamp and compare it with the expected Zeeman splittings. Assume the temperature of the emitting vapor is 500 K.
6. Derive a formula for  $e/m$  in terms of the measured separations of identified peaks in the interferogram of the Zeeman pattern, the distance between the plates of the interferometer, the strength of the magnetic field, and various physical constants.

### QUANTITIES YOU WILL DETERMINE

1. The Zeeman splittings of the green and yellow lines of mercury and the green line (5400 Å) of neon.
2. The Landé  $g$ -factors for the levels involved in mercury lines.

3. The value of  $e/m$  for the electron.
4. The hyperfine structure of the mercury 5461 Å line.
5. The isotope shift (effect of nuclear mass) of the 5461 Å lines of the even isotopes of mercury.

## INTRODUCTION

Since Faraday's discovery in 1848 of magnetically induced circular birefringence (the Faraday Effect), the search for effects of electric and magnetic fields on optical phenomena has been pursued with more and more powerful methods of spectroscopy and stronger and stronger fields. In 1862, in his last experimental work, Faraday himself used the most powerful magnet and best prism spectroscope available in an unsuccessful attempt to detect an effect of a magnetic field on the spectral lines emitted by sodium vapor in a Bunsen burner flame.

Three decades later Pieter Zeeman in Leyden, unaware of Faraday's earlier attempt, was induced "by reasons of minor importance" to try to detect a magnetically induced change in the light of a sodium flame. He too failed. However, as Zeeman describes it in his discovery paper of 1896 (reproduced in Appendix A) his attention was subsequently drawn to Maxwell's sketch of Faraday's life in which Faraday's last experiment is mentioned. Zeeman wrote "If a Faraday thought of the possibility of the above mentioned relation, perhaps it might be yet worth while to try the experiment again with the excellent auxiliaries of spectroscopy of the present time." Using a grating ruled on the marvelous engine of Rowland at Johns Hopkins he observed a broadening of the spectral lines emitted by sodium vapor heated in a flame between the poles of a powerful Ruhmkorff magnet which produced a field of 10 kilogauss.

Zeeman proposed a theoretical interpretation based on Lorentz's idea that "in all bodies small electrically charged particles with a definite mass are present." Given this concept, the rest of the interpretation is, from a modern point of view, hardly more than a dimensional analysis. Nevertheless this early theory of the "normal" Zeeman effect showed how to interpret the observed line broadening as a measure of  $e/m$ , the charge to mass ratio of the electron. The idea was that the frequency of a spectral line emitted by an atom is the frequency of a harmonic vibration of an electron in the atom. Any such vibration can be resolved into two components, one along some particular direction which we take to be the direction of the  $z$  axis, and the other in the  $xy$  plane. The  $xy$  component, in turn, can be represented as the sum of two components of constant amplitude rotating in opposite directions about the  $z$  axis. With each such circular component of motion one can associate a central restraining force given by

$$F = mr\omega^2, \tag{1}$$

where  $\omega$  is the angular frequency and  $r$  is the radius of the circular motion. If a magnetic field of

magnitude  $B$  is now imposed in the  $z$  direction, the central force will be either increased or decreased by a perturbing (i.e small compared to  $F$ ) Lorentz force of magnitude  $Be\omega r/c$  (cgs units), resulting in a changed frequency of circular motion given by the equation

$$mr(\omega \pm \omega)^2 = F \pm \frac{Be\omega r}{c}, \quad (2)$$

or

$$mr[\omega^2 + 2\omega \pm \omega + (\pm \omega)^2] = mr\omega^2 \pm \frac{Be\omega r}{c}. \quad (3)$$

Neglecting the  $(\pm \omega)^2$  term, one obtains the simple expression

$$\omega \pm \omega = \omega \pm \frac{Be}{2mc} \quad (4)$$

for the frequencies of light viewed along the direction of the field (as viewed through a hole bored through the magnet pole piece). In directions perpendicular to the field, one sees both these shifted frequencies and the unshifted frequency of the components of vibration along the  $z$  axis which, being parallel to the field, is unaffected. With the resolution available to Zeeman the individual frequency-shifted lines were unresolved. However, Lorentz pointed out to Zeeman that the edges of the broadened lines observed parallel to the field, supposedly being light radiated by charges in right and left circular motions, should exhibit circular polarization in opposite senses with respect to one another. With a quarter wave plate and Nicol prism polarizer Zeeman confirmed the prediction. And by rough estimation of  $\omega$  and knowledge of  $B$  he obtained a value of  $10^7$  emu for  $e/m$ .

Within a few months of Zeeman's publication magnetically split lines were spectroscopically resolved and found in many cases to consist of more than the "normal" Zeeman triplet, and to have frequency shifts other than  $\pm Be/2mc$ . The "anomalous" Zeeman effect, which proved to be the rule and not the exception, defied explanation until the advent of quantum mechanics and the discovery of spin.

A modern understanding of the Zeeman effect can be approached on several levels. The vector model, which you should master before starting the experiment, is explained in Melissinos (1966) and in various texts on quantum mechanics and atomic structure listed in the references. It provides a useful image of the atomic machinery involved in the Zeeman effect and yields accurate predictions of the Zeeman effect in atoms whose excited states can be described according to the LS coupling scheme (Russell-Saunders coupling). Information about the mercury spectrum in general and the Zeeman effect on the green and yellow lines of mercury can also be found in Melissinos. (Beware of errors in

Melissinos description of the hyperfine structure of the mercury lines.) Specially useful references are the classic work on atomic spectra by White (1934), and a recent book by Steinfeld (1986).

### EXPERIMENTAL ARRANGEMENT

In this experiment you will measure the weak-field Zeeman effect on the green and yellow lines of mercury and the green line of neon by means of a Fabry-Perot interferometer. This device provides the high spectral resolution necessary for the detection and measurement of the small fractional changes in wavelength caused by "weak" magnetic fields of several thousands of gauss. The results reveal some of the important phenomenology of angular momenta, spin, and the dipole selection rules, as well as an accurate value of  $e/m$  from an interpretation of the data based on the vector model for the quantum mechanical addition of angular momentum. In addition, with sufficient care in the adjustment of the apparatus you can detect and measure the hyperfine structure of the green line of the odd isotopes of mercury due to the interactions between the electronic and nuclear magnetic moments, and the spread in wavelength of the lines of the even isotopes due to the differences in the number of neutrons in their nuclei.

The optical arrangement is illustrated in Figure 1. Light emitted by a low-pressure mercury

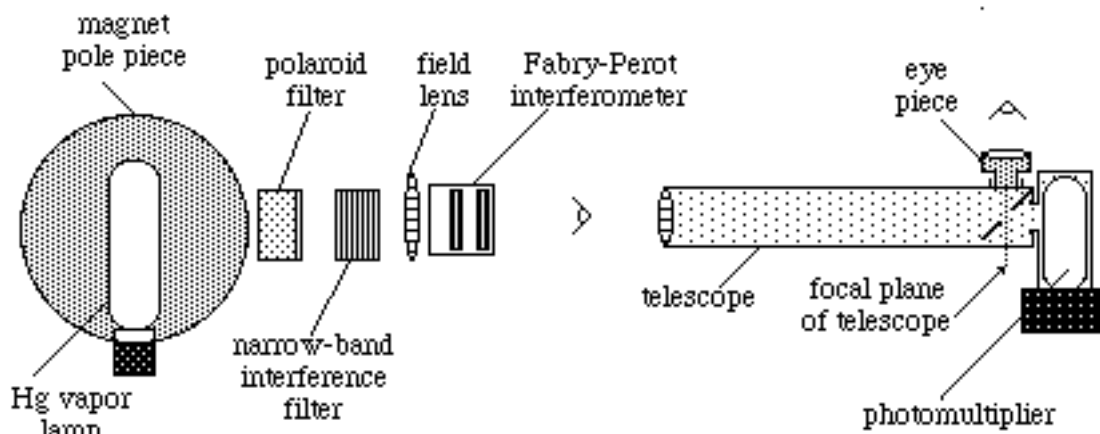


Figure 1. Schematic diagram of the optical arrangement for recording the intensity at the center of the Fabry-Perot interferogram

vapor lamp passes through a narrow-band interference filter, an optional Polaroid filter, a field lens, the Fabry-Perot interferometer, and a telescope. When properly aligned this system produces at the focal plane of the telescope objective lens interference fringes in the form of circular rings concentric with the axis. A 45°-degree front-aluminized mirror with a small hole in the aluminization centered on the focal plane reflects most of the ring pattern for viewing through the eyepiece, while allowing the light at the center "bull's eye" of the ring pattern to pass through to the photomultiplier. During a spectrum scan the

separation of the Fabry-Perot plates is varied by two or three wavelengths by application of a saw-tooth voltage with an amplitude of several hundred volts to three piezoelectric crystals on which one of the plates is mounted. As the separation decreases (increases) the rings in the image plane expand (contract). A plot of the intensity of light passing through the hole located at the center of the ring pattern against the magnitude of the saw-tooth voltage is, in effect, an ultra-high resolution spectrum over a very narrow range of frequencies.

Figure 2 shows the electronic arrangement for recording the central intensity as a function of the voltage applied to the piezoelectric crystal. The photomultiplier output is fed directly to the Y input of an oscilloscope operating in an X-Y plotter mode. A signal proportional to the voltage applied to the piezoelectric crystals is fed from the interferometer controller to the X input of the oscilloscope.

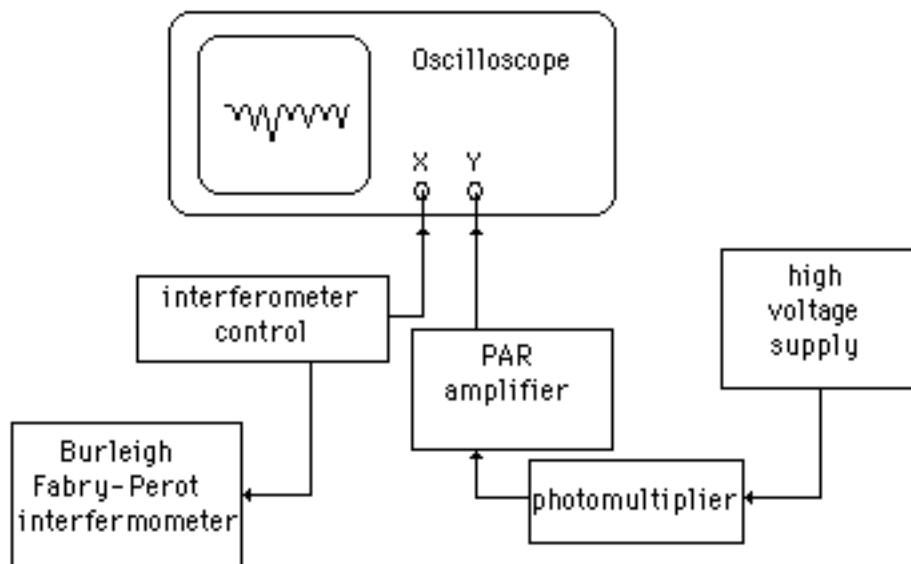


Figure 2. Schematic diagram of the electronic arrangement for recording the interferogram in the form of a plot of the central intensity versus the separation of the FP plates.

### Theory of the Fabry-Perot Interferometer

A Fabry-Perot interferometer (FP) consists of two precisely parallel glass plates with optically flat and highly reflective surfaces facing one another, as illustrated in Figure 3. To use it as a spectrometer one must have, in addition, a lens to focus parallel rays to a point in its image plane and a magnifying eyepiece for examining the intensity pattern of light in the focal plane, i.e. a telescope.

Consider a ray of light of wavelength  $\lambda$ , emitted by an excited mercury atom at S and making an angle  $\theta$  with the axis, is incident on the FP from the left at the point A. It will be partially transmitted

at each of the two FP mirror surfaces, and will arrive at P after passing through the telescope lens. The portion of the ray reflected at B will be reflected again at C and partially transmitted at E. It will enter the telescope lens parallel to the original ray and will be focussed to the same point P after having traversed an additional distance  $2D \cos\theta$ . If this additional distance is an integer number of wavelengths, i.e.,

$$2D\cos\theta = m\lambda, \quad (5)$$

then the two rays (and all the additional multiply reflected rays) will interfere constructively when brought to the focus at P. Constructive interference among all the multiply reflected rays passing through the interferometer at an angle  $\theta$  to the axis will produce a circle of interference maxima in the focal plane, i.e., a bright ring of the  $m$ th order of interference. If the separation of the plates is increased, then the angular radius of the  $m$ th order ring will expand so that the decrease in  $\cos\theta$  compensates for the increase in  $D$ .

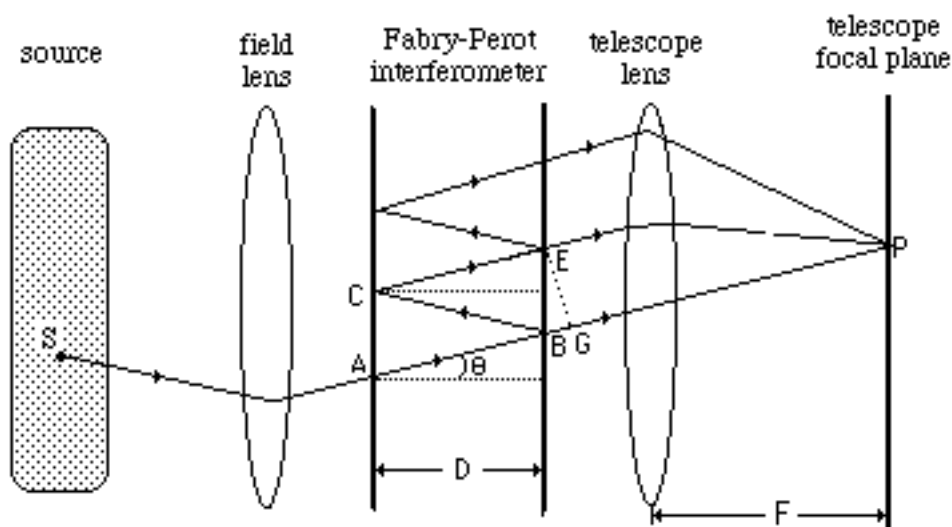


Figure 3. Geometrical optics of the Fabry-Perot interferometer. Only one of many multiply reflected paths is shown.

Suppose you want to measure the difference  $\delta\lambda$  between two wavelengths very close together, e.g., the wavelength shift between two lines in a Zeeman pattern. Suppose, further, that the average wavelength  $\lambda$  of the two lines is already known to good accuracy. Viewing the light emerging from the interferometer with your naked eye or through a telescope focused on infinity, you will see two concentric sets of interference rings, corresponding to the two wavelengths. Suppose the  $m$ th order ring of wavelength  $\lambda_1$  coincides with a fiducial mark fixed in the focal plane (e.g. a dirt spot on the  $45^\circ$  mirror in

the Junior Lab setup). Call  $\delta D$  the change in mirror separation required to bring the  $m$ th order ring of wavelength  $\lambda_1 + \delta\lambda$  into coincidence with the fiducial mark. According to equation (5)

$$\delta D = m\delta\lambda / (2\cos\theta). \quad (6)$$

Call  $D$  the change in mirror separation required to bring the  $m + 1$  ring of wavelength  $\lambda_1$  into coincidence with the same fiducial mark. In this case

$$D = \lambda_1 / (2\cos\theta). \quad (7)$$

Combining equations (5), (6) and (7) and setting  $\cos\theta = 1$  (an accurate approximation since  $\theta \ll 1$ ) we obtain

$$\delta\lambda = \lambda(\lambda/D)(\delta D/D) \quad (8)$$

which is an expression for the desired wavelength difference in terms of the known wavelength  $\lambda$ , the mirror separation, and the *ratio* of the changes in separation of the mirrors. In practice the changes can be measured as differences in the digital readings of the bias meter on the Burleigh controller. Since the latter are proportional to the actual changes in mirror separation, the ratio of the meter differences is equal to the ratio of the actual separation changes.

From equation (8) one can see that if  $\delta\lambda = \lambda(\lambda/2D) = \lambda/m$ , then  $\delta D = D$ , i.e., the mirror movement required to shift the ring pattern from the  $m$ th order ring of wavelength  $\lambda$  to the same order ring of wavelength  $\lambda + \delta\lambda$  would be the same as the movement required to shift the pattern from the  $m$ th order ring of  $\lambda$  to the ring of order  $m+1$  of the same wavelength. The quantity  $\lambda/m$  is called the free spectral range of the instrument for a particular separation of the mirrors. It represents the difference between two wavelengths such that the  $m$ th interference maximum of the larger wavelength coincides with the  $(m+1)$  maximum of the smaller wavelength, i.e.  $(m+1)\lambda = m(\lambda + \lambda/m)$ . To avoid confusion as to which interference order a given feature of a complex line may belong, it is generally wise to adopt a mirror separation that gives a free spectral range larger than the wavelength difference to be measured.

The effectiveness of a Fabry-Perot interferometer for high-resolution spectroscopy depends critically on the reflectivity of its mirrors - the higher the reflectivity the sharper, or narrower, the lines. To quantify this relation one must consider the combined effects of the reflection coefficient and additional path length on the contribution that each transmitted beam makes to the total complex amplitude of the optical disturbance at P. If we call  $r$  the amplitude reflection coefficient, then the factor by which the amplitude of the ray emerging at E is reduced relative to the direct ray is  $r^2$ . In addition the ray is

retarded in phase by the angle

$$\alpha = \frac{4D}{\lambda} \cos\theta \quad . \quad (9)$$

Similarly, the  $n^{\text{th}}$  multiply reflected ray will arrive at P attenuated by the factor  $(r^2)^n$  and retarded in phase by  $n\alpha$ . If the amplitude at P of the wave arriving by the direct path is  $A \exp[j(\omega t + \phi)]$ , then the total amplitude at P is the complex quantity

$$A_{\text{tot}} = A \exp[j(\omega t + \phi)] \{ 1 + r^2 \exp(-j\alpha) + [r^2 \exp(-j\alpha)]^2 + [r^2 \exp(-j\alpha)]^3 + \dots \} . \quad (10)$$

This is a geometric series of which the sum is

$$A_{\text{tot}} = \frac{A \exp[j(\omega t + \phi)]}{1 - r^2 \exp(-j\alpha)} . \quad (11)$$

The intensity at P is proportional to the square of the magnitude of  $A_{\text{tot}}$  which we obtain by multiplying  $A_{\text{tot}}$  by its complex conjugate. The ratio of this intensity to the intensity at the center where  $\theta=0$  is then

$$\frac{I}{I_0} = \frac{(1 - R)^2}{1 - 2R \cos\alpha + R^2} , \quad (12)$$

where we have replaced  $r^2$  by  $R$ , the intensity reflectivity of the surfaces. At any fixed wavelength and plate separation  $\alpha$  depends only on the position of P in the focal plane of the telescope lens and not on the position of S. Thus the ratio of the sum of the contributions to the intensity at P from all the incoherent atomic sources in the lamp to the sum at the center of the focused ring pattern is given by equation (12) which is, therefore, the general formula for the intensity in the focal plane.

The maxima of the intensity occur where  $\alpha/2 = (2D/\lambda) \cos\theta = m$ , where  $m$  is an integer called the order of the interference. Changes in the value of  $\alpha/2$  are related to changes in  $D$ ,  $\lambda$  and  $\theta$  by the differential relation

$$\left( \frac{\alpha}{2} \right) = \frac{2\cos\theta}{\lambda} \delta D - \frac{2D\cos\theta}{\lambda^2} \delta\lambda - \frac{2D\sin\theta}{\lambda} \delta\theta . \quad (13)$$

At the center (bull's eye) of the interference ring pattern, where  $\cos\theta = 1$ , the order of interference can be

changed from  $m$  to  $m+1$  either by increasing  $D$  by  $D = \lambda/2$  or by decreasing  $\lambda$  by  $\lambda = (\lambda/2D)\lambda = \lambda/m$ . As mentioned previously, quantity  $\lambda$  is called the free spectral range. It is the maximum width of the Zeeman pattern of a given order of interference that can be displayed without overlapping the patterns of the adjacent orders. To express the free spectral range in terms of wave numbers (reciprocal wavelength) one use the relation

$$|\Delta(1/\lambda)| = (1/\lambda^2) \Delta\lambda = 1/(2D). \quad (14)$$

In a typical setup  $D = 0.25$  cm,  $\lambda = 5000$  Å,  $m = 10,000$ , and the free spectral range in wavenumbers is  $(2D)^{-1} = 2.0$  cm<sup>-1</sup>.

To see what equation (12) tells about how the intensity depends on very small displacements of the plates and on very small changes of the wavelength, we define two dimensionless parameters  $f$  and  $g$  such that  $D = (1+f)m_0\lambda_0/2$  and  $\lambda = (1+g)\lambda_0$ . The parameter  $f$  measures the change in separation of the plates in units of  $\lambda_0/2$  and is of the order of  $1/m_0$ . We will be interested in the effects of very small changes in wavelength for which typical values of  $g$  are also of the order  $1/m_0$  so that  $1/(1+g)$  can be approximated to high accuracy by  $(1-g)$ . In practical setups  $\theta < 1^\circ$  so that we can replace  $\cos\theta$  by the approximation  $(1-\theta^2/2)$ . Substituting the expressions for  $D$  and  $\lambda$  with these approximations in equations (6) and (7) and dropping the terms of negligible smallness, we obtain

$$\frac{I}{I_0} = \frac{(1-R)^2}{1 - 2R \cos[(2(f-g-\theta^2/2))] + R^2} \quad (15)$$

Figure 4 is a plot of the intensity versus angle in the interferograms formed by a FP with  $m_0 = 24,818$  and  $R = 0.8$ , illuminated by light with two wavelengths,  $\lambda_1 = 5461$  Å and  $\lambda_2 = \lambda_1(1+5 \times 10^{-6})$ . The four sets of curves are for four different values of the plate separation. The dashed lines are the separate intensity curves for the two wavelengths, and the solid line is their sum. Figure 5 shows the summed intensities versus angle for the same FP and wavelengths, but for four different reflectivities. Figure 6 shows plots of the intensity at the center of the interferogram ( $\theta = 0$ ) as functions of the plate separation for four reflectivities. This is the form of the interferogram/spectrogram you will record in the present experiment.

The intensity function has maxima in the focal plane on concentric circles to which are focused rays leaving the FP at angles  $\theta$  such that  $(2D\lambda)\cos\theta = m$ , where  $m$  is an integer. Since we are dealing with small angles we again use the approximation  $\cos\theta = (1-\theta^2/2)$ . If  $2D\lambda = m_0$ , the  $m$ th maximum will lie at the angles  $\theta_m = [2(m_0 - m)/m_0]^{1/2}$ .

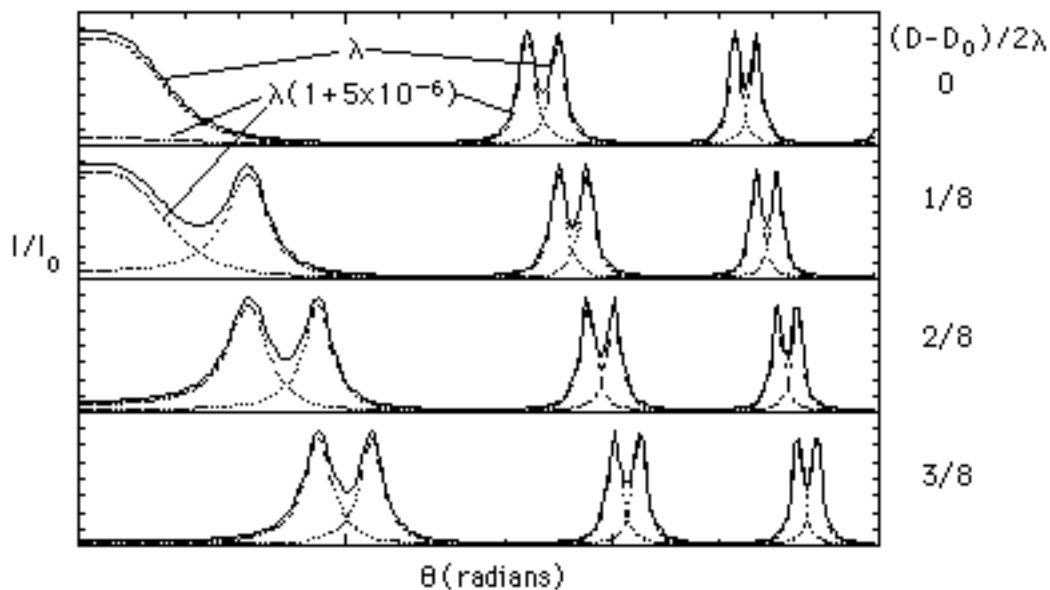


Figure 4. Plot of intensity against angle in theoretical interferograms of two wavelengths differing in wavelength by 5 parts in a million produced by a FP with  $2D_0/\lambda_0 \sim 24,818$ , and reflectivity  $R=0.8$ . The four plots are for four successively larger plate separations, the first differing from the fourth by  $3/8\lambda$ .

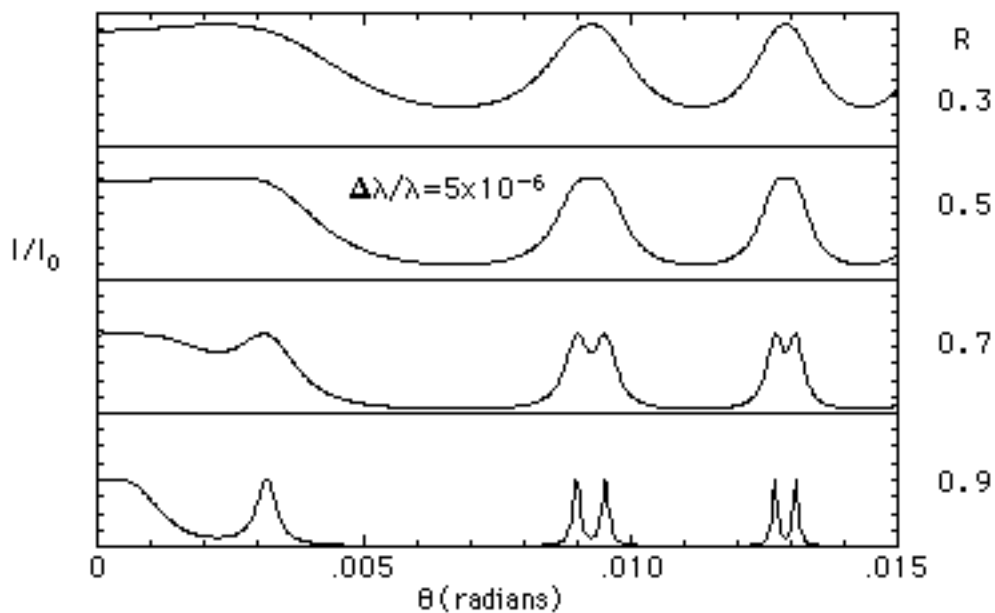


Figure 5. Plot of intensity against angle in interferograms of light containing two wavelengths, for various reflectivities.

We now ask "By how much must the phase factor  $\alpha = (4 D/\lambda)\cos\theta$  change to decrease the intensity from a maximum value to half maximum?". Remembering that at a maximum the phase factor is an integral multiple of  $2\pi$ , and using the identity  $\cos(2\pi n + \delta\alpha) = \cos(\delta\alpha)$ , we have from (12) the relation

$$\frac{(1 - R)^2}{1 - 2R \cos(\delta\alpha) + R^2} = \frac{1}{2}, \tag{16}$$

from which we obtain

$$\cos(\delta\alpha) = 1 - \frac{(1 - R)^2}{2R}, \tag{17}$$

or, to a good approximation

$$\delta\alpha = \frac{(1 - R)}{R^{1/2}}. \tag{18}$$

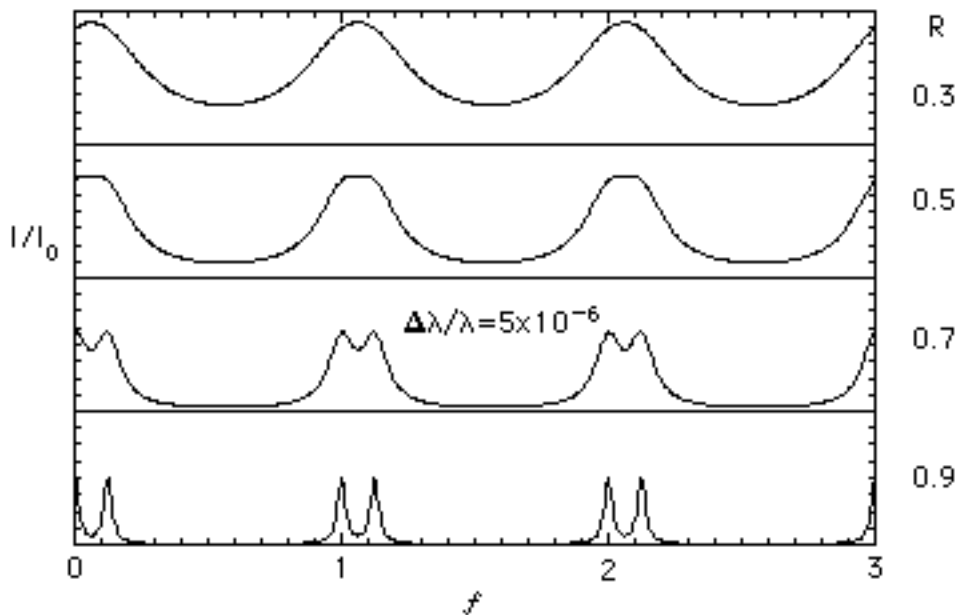


Figure 6. Plot of intensity at the center of the interferogram (the bull's eye) against the separation of the Fabry-Perot mirrors for various reflectivities.

If we measure the intensity at  $\theta = 0$  as a function of the separation, then the change in  $D$  to the half intensity point is

$$\delta D = (\lambda/4) (1-R)/R^{1/2} . \quad (19)$$

The change in  $D$  between successive maxima is  $\lambda/2$ . Thus the resolution of the interferometer, defined as the ratio of these quantities and called the finesse, is

$$\text{finesse} = 2 R^{1/2}/(1-R). \quad (20)$$

## PROCEDURE

### 1. Align the interferometer

The Burleigh Fabry-Perot interferometer is a delicate and expensive (\$6000) instrument capable of providing spectrum measurements of extraordinary resolution and precision. Please treat it with the utmost care. In particular, do not press the mirrors together by turning the micrometer screws below 0 as you may crack the sapphire blocks on which the micrometer crews press. If you encounter any problems or are uncertain how to adjust the interferometer, call for assistance.

Mount the mercury-filled Geisler tube in the sockets of the high-voltage supply, position the capillary section between the pole pieces, and turn it on. Adjust the collimating lens and the position and orientation of the interferometer so that the light falls on the input mirror and the view through the FP mirrors looking toward the lamp is fully illuminated. Put the interference filter for the 5461 Å green line of mercury in the beam. Set the two positioning micrometers on scale readings of 0.200 cm. (Do not move the left mirror.) Make the mirrors parallel by adjusting the bottom micrometer (which has no scale) and top right micrometer while viewing the light coming through the FP mirrors. When the mirrors are nearly parallel you will see many narrow circular fringes. Fine adjustment will produce comparatively large, sharp circular fringes concentric with the center of your field of view and separated by dark gaps with fainter and narrower rings. When the mirrors are perfectly parallel the circular fringes are sharp and do not change in diameter as you move your eye back-and-forth, and up-and-down.

### 2. Align the telescope.

Check that the mirror mounted inside the telescope under the eyepiece is inclined at an angle of 45° so that it reflects the light from the telescope lens into the eyepiece. Focus the eyepiece on the tiny aperture (a ragged laser-drilled hole in the aluminization near the center of the mirror). Then point the telescope at a distant object and focus it by adjusting the slide tube.

Place the telescope so that the light emerging from the interferometer enters the objective lens. (Leave sufficient room between the telescope and the interferometer to insert your head for direct viewing of the interference fringes). Adjust the orientation of the telescope so that the circular fringes seen through the eyepiece are concentric with the tiny aperture in the 45° mirror. (The broad rings are successive orders of interference of the light from the even isotopes of mercury: the breadth of the line is

due to the effect of the spread in mass of the isotopes. The faint, narrow rings between the broad ones are the hyperfine lines of the odd isotopes, separated slightly in wavelength from the others as a result of the interaction between the nuclear and electronic magnetic moments.)

### 3. Adjust the FP controller.

Turn on the controller and explore its operation with the help of the diagram in Figure 7 and the instrument manual. The function of the controller is to supply a sawtooth voltage to each of three piezoelectric crystals on which the input (left) FP mirror is mounted. The duration and amplitude of the sawtooth voltages are controlled by the correspondingly labeled knobs. The ramp bias knob controls the voltage level of the midpoint of the scan voltage applied to all three crystals; the three bias controls on the left adjust the mean voltages applied to each crystal. The trim controls adjust the slopes of the sawtooth voltages to compensate for any differences that may exist in the electromechanical properties of the crystals.

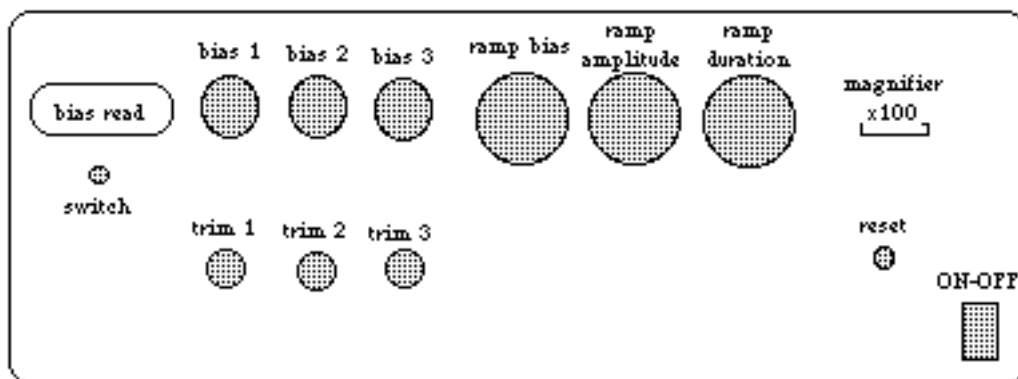


Figure 7. Diagram of the front panel of the interferometer controller. Note that the knobs are friction-coupled to their shafts so that they turn past the zero and maximum positions without harm.

With the ramp amplitude turned to zero, set the three bias controls and the three trim controls to near their middle values. Application of the bias voltages to the piezoelectric crystal mounts of the input mirror will disturb the parallelism. So, once again, view the fringes directly with your eye close to the output mirror of the interferometer and make the mirrors parallel by adjusting the bottom and top right micrometers. Now view the fringe pattern through the telescope and tweak the bias controls for maximum sharpness. Adjust the telescope orientation so that the aperture hole is exactly at the bull's eye of the circular fringe pattern. You can shift the fringe pattern by adjusting the ramp bias control.

#### 4. Display the spectrum.

Put the photomultiplier in its place at the end of the telescope and turn up the PM high voltage to  $\sim 1400$  v. Feed the signal from the PM to the PAR amplifier with the LF rolloff control set to DC, and the HF rolloff set to 3 Hz. Display the output on the y-axis of the digital oscilloscope operating in the X-Y mode with the scan signal from the FP controller connected to the X-display. Adjust the scan amplitude so that the piezoelectric drive is activated. Select a bias sweep amplitude and repetition rate that produces a pleasing display of the variation of light intensity at the bullseye of the interferometer pattern over a range of two or three free spectral ranges. Adjust the three bias controls to maximize the amplitudes of the peaks.

Observe the pattern and identify the hyperfine lines with the help of the plot copied from the American Institute of Physics Handbook and posted on the wall.

#### 5. Determine the offset of the micrometer scale

The position of the fixed left mirror mount has been set so that zero readings of the micrometers correspond to a small positive mirror separation which we call the offset,  $D_0$ . Accurate knowledge of this offset is obviously required so that micrometer readings can be converted into actual mirror separations according to the equation

$$D = D_0 + r, \quad (21)$$

where  $r$  is the micrometer reading (we will assume that the micrometers are accurately manufactured so that one turn equals .025 cm and the smallest scale division on the barrels is .050 cm). The offset can be determined without mechanically measuring the separation of the mirrors, which is difficult at best and would likely damage the reflective surfaces of the mirrors. (Do not move the left mirror.) To see how to measure the offset, consider two close spectral lines with wavelengths  $\lambda_1$  and  $\lambda_2$  such that

$$(\lambda_2 - \lambda_1) \ll (\lambda_2 + \lambda_1)/2.$$

(In practice one can use two of the narrow hyperfine lines of mercury 5461 Å, preferably the two brightest hyperfine lines on either side of the central broad line which is composed of the unresolved isotope-shifted lines of the mercury isotopes with even numbers of nucleons and protons in their nuclei). Call  $r_1$  and  $r_2$  the micrometer readings for two settings of the movable mirror (e.g.  $r_1 = 0.200$  cm and  $r_2 = 0.400$  cm). Suppose the separation between the interference maxima of the two lines in a given order is  $\Delta_1$  at the  $r_1$  and  $\Delta_2$  at the  $r_2$  setting. The separations can be measured as the differences between the

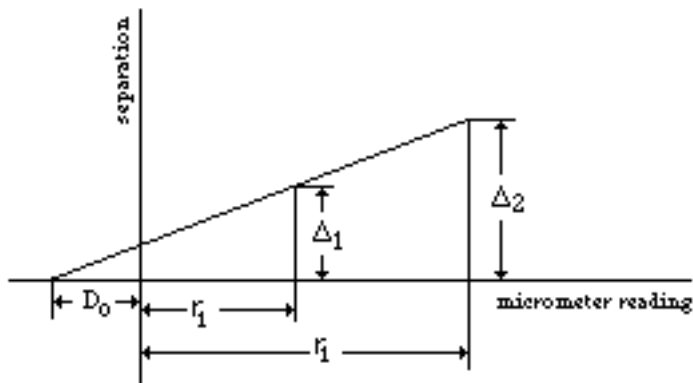


Figure 8. Schematic plot of the separation against the micrometer reading in the determination of the micrometer offset  $D_0$ .

bias readings on the FP controller required to bring first one and then the other of the interference rings of  $\lambda_1$  and  $\lambda_2$  (in the same order of interference) to the same fiducial radius in the interferogram as marked by a dust spot on the  $45^\circ$  mirror in the focal plane of the telescope, as explained previously. A straight line fitted to a plot of  $\Delta$  against  $r$  will intercept the  $r$ -axis at  $d_0$ . To achieve confidence and good accuracy in this measurement on which the accuracy of the final results depends, it is wise measure several times ( $\geq 5$ ) at each of several micrometer settings, say 0.0, 1.0, 2.0, 3.0, 4.0 mm.

#### 6. Estimate the optimum mirror separation.

Calculate the separation between the FP mirrors which will provide a "free spectral range" suitable for the desired measurements. What you want to avoid is having the extreme red-shifted Zeeman components of a given line in one order of interference overlap the extreme blue-shifted components of the line in the next order when the field is at maximum strength. Estimate the total width of the Zeeman pattern that you expect at the maximum attainable field strength. Calculate the mirror separation which will give you the necessary free spectral range to accommodate this width. Allowing for the micrometer offset determined above, set the desired mirror separation.

#### 7. Trial runs.

Turn on the magnet water supply (faucet on the right rear wall of the room) and then the power supply (located under the table). Observe the fringe pattern through the telescope as you increase the magnet current. Note the behavior of the hyperfine lines. Test the effect on the fringe pattern of inserting a Polaroid filter in the optical path between the source lamp and the FP. Rotate the Polaroid and figure out what is happening. (You can determine the transmission axis of the Polaroid filter by observing light reflected at small angles of grazing incidence from any non-metallic glossy surface like that of the table in

the next room.)

When everything is properly adjusted, with the bull's eye of the interference pattern centered on the hole in the  $45^\circ$  mirror and with the bull's eye intensity signal displayed on the oscilloscope, a pattern similar to that in Figure 6 with  $R \sim 0.9$  should be seen.

## 8. Measurements

### Zeeman effect on the green line of mercury

Using the Hall probe magnetometer explore and record, as a function of the supply current, the intensity of the field between the pole pieces of the magnet in the region that will be occupied by the mercury vapor and up against the centers of the faces of the pole pieces. (Check the Hall magnetometer zero setting by inserting the probe into the magnetically shielded cavity provided, and check the calibration with the 5 kilogauss standard magnet, also provided.)

Readjust the interferometer, and measure the Zeeman splittings. As suggested above, the most convenient way to measure the Zeeman splittings is to record the digital reading of the ramp bias required to move the various interference rings seen in the telescope to a chosen fiducial position marked by a dirt spot on the  $45^\circ$  mirror at the focal plane of the telescope. To do this first stop the scanning action by turning the ramp amplitude to zero. Then select a dirt spot on the mirror at some as your fiducial marker. Adjust the ramp bias control so the spot is on the center line of an interference ring of a particular reference spectrum line, and record the bias reading. Repeat for the other rings of the same order of interference for the spectrum lines whose wavelength shift relative to the reference line you wish to measure. Also record the bias readings for interference rings in several adjacent orders to establish the calibration scale and to provide redundant data from which the random measurement errors can be evaluated. Although this procedure will provide you with all the necessary data in the easiest and most accurate way, it is a good idea to record the spectrum photographically as described above so you will have a record of what you measured.

### Isotope and hyperfine structure of the 5461 Å line

At zero field tweak up the performance of the interferometer with the bias controls to sharpen up as much as you can the hyperfine components of the green line which appear as the faint, sharper rings between the bright, broad rings of the unresolved emission from the even isotopes. Increase the gain of the oscilloscope Y amplifier to make the hyperfine peaks large enough to be accurately measurable when photographed. Photograph the oscilloscope display of the interferogram. Here again you can obtain all the necessary measurements using the ramp bias control. Measure a second interferogram with the mirror separation changed to another precisely measured value about 10% different from the first. The resulting changes in the relative positions of the hyperfine lines will provide essential clues to their identifications.

Beware of confusing interference rings of different orders.

### The yellow doublet lines of mercury

To observe the mercury yellow lines remove the green interference filter from the optical path and insert the yellow interference filter mounted in the heavy brass cylinder into the output hole of the interferometer. Note that there will now be two sets of interference rings present since the filter passes both of the yellow lines. With luck the two sets of rings may be conveniently spaced so that their Zeeman patterns do not overlap at moderate fields. If not, you will have to change the spacing of the mirrors slightly.

Measure the structure and splitting of both components of the mercury yellow doublet. This will require special care because of possible overlapping of the two interference patterns at high field values. Note the slight difference in the Zeeman patterns of the 5769.6 Å and 5461 Å lines. How do they differ and why?

### The green line of neon

The energy level structure of neon is much more complicated than that of mercury, and the interpretation of the Zeeman patterns of its spectrum is difficult, to say the least. In the ground state the outer 6 electrons are in a closed 2p shell. The transitions that give rise to the spectacular visible spectrum of ordinary neon discharge tubes are between excited states in which one electron has been raised from one of the 2p orbitals. The excited states consist of various configurations of that electron and of the 5 electrons remaining in the 2p shell. It turns out that the interactions between the orbit and spin moments of the excited electron and the remaining 2p electrons cannot be described by the LS coupling approximation (Russell-Saunders coupling), but rather as jj coupling, which does not lend itself to a simple vector-model calculation of the  $g$ -factors. The purpose of this part of the experiment is therefore limited to measuring the pattern of one particularly prominent and accessible line of the neon spectrum (the relatively intense green line at 5401 Å), and to comparing the splitting with the simple classical Zeeman triplet.

It happens that the 5401 Å line is transmitted by the same green filter used to isolate the 5461 Å line of mercury. To observe it, restore the green interference filter and replace the mercury lamp between the magnet pole pieces with the small neon lamp. The latter has its own separate power supply and no need for cooling. The transmitted intensity of this neon line is rather faint because it lies close to the edge of the filter's transmission band. Considerable skill will be required to obtain a useful measure of its Zeeman pattern.

### ANALYSIS

To check the results of your ramp bias measurements of the Zeeman splittings you can measure the separations on the photographic records between the peaks of the interferograms with the traveling stage microscope set up in Room 4-310. Be sure to measure the separation between the same Zeeman components in adjacent orders, i.e. the distance in the photograph corresponding to the free spectral range. From these quantities and the separation of the mirrors of the Fabry-Perot interferometer, compute the effective dispersion of the spectroscopy, i.e. the shift in wavenumber per unit distance on the photographs.

Measurements made with the ramp bias control are analyzed in the same fashion as those made from the photographic records.

Tabulate all the measured frequency shifts in units of wave numbers ( $\nu/c$ ) = (1/ ) per kilogauss, e.g. (0.1234±0.012) cm<sup>-1</sup>Kg<sup>-1</sup>.

Construct energy level diagrams of the mercury transitions and identify the observed Zeeman component frequencies with the various allowed transitions between the magnetic substates.

Measure the hyperfine lines, and identify them with the help of the discussion by Steinfeld (1986). (Some of the illustrations and diagrams in Melissinos on this topic are in error.)

Measure the full width at half maximum of a strong hyperfine line to obtain a measure of the effective resolution of the spectrometry. Measure the FWHM of the bright, unresolved composite line of the even isotopes. Derive from these data a measure of the spread in wavelengths of the even isotope lines due to the differences in their nuclear masses. Can you think of a way to make an order of magnitude theoretical prediction of this spread?

Compute the Landé  $g$ -factors for the upper and lower states involved in the various transitions (Hg 5461 Å, Hg 5770-5790 Å and the magnetic moments of each of the levels in units of the Bohr magneton.

If everything makes sense, i.e. all the measured shifts of the  $\pi$  and  $\sigma$  components are consistent with expectations derived from the vector model and selection rules, then determine a best value for  $e/m$  for the entire data set.

Finally, compare the neon splitting with the classical triplet splitting. You may want to search the literature for a theoretical analysis of the neon spectrum and its Zeeman splittings.

Estimate the random and systematic errors associated with each of your final quantitative conclusions.

## REFERENCES AND BIBLIOGRAPHY

- E.U. Condon and G. Shortley, *The Theory of Atomic Spectra* (Cambridge, 1959).
- L.D. Landau and E.M. Lifshitz, *Quantum Mechanics* (Pergamon, 1974).
- A. Melissinos, *Experiments in Modern Physics* (Academic Press, 1966), Chapter 7.
- E. Merzbacher, *Quantum Mechanics* (Wiley, 1961).
- F.K. Richtmyer, E.H. Kennard, and T. Lauritsen, *Introduction to Modern Physics* (McGraw-Hill, 1955), p.291.
- B. B. Rossi, *Optics* (Addison-Wesley, 1957), p.140.
- H. Semat, *Introduction to Atomic and Nuclear Physics* (Holt, Rinehart and Winston, 1962), p. 291.
- J. Steinfeld, *Molecules and Radiation* (MIT Press 1986) (In Junior Lab Library and Hayden).
- H. E. White, *Introduction to Atomic Spectra* (McGraw-Hill, 1934).

#### SUGGESTED THEORETICAL TOPICS

1. The vector model and the Landé g-factor.
2. Hyperfine structure.
3. The isotope shift.
4. The physical optics of the Fabry-Perot interferometer.

#### Appendix A

Dr. P. Zeeman on the Influence of Magnetism on the Nature of Light emitted by a Substance.

Phil. Mag., vol. 43, p. 226 (1897)